https://doi.org/10.20965/jrm.2023.p1135

Paper:

Difference in the Osteoblastic Calcium Signaling Response Between Compression and Stretching Mechanical Stimuli

Katsuya Sato*, Tasuku Nakahara, and Kazuyuki Minami****

*Graduate School of Technology, Industrial and Social Sciences, Tokushima University
2-1 Minamijosanjima, Tokushima 770-8506, Japan
E-mail: katsuyas@tokushima-u.ac.jp
**Graduate School of Science and Technology for Innovation, Yamaguchi University
2-16-1 Tokiwadai, Ube, Yamaguchi 755-8611, Japan
[Received March 20, 2023; accepted July 4, 2023]

In orthodontics, various forms of mechanical stimulation induce opposing bone metabolism mechanisms. Bone resorption and bone formation occur in areas of compressive and tensile force action, respectively. The mechanism that causes such a difference in bone metabolism is still unclear. In this study, we investigated the difference in the osteoblastic calcium signaling response between compression and stretching mechanical stimuli. We applied two types of mechanical stimuli to osteoblast-like MC3T3-E1 cells: first microneedle direct indentation onto the cell as compression stimuli, and second stretching stimuli by using originally developed cell stretching MEMS device. Cells were treated with thapsigargin and calcium-free medium to investigate the source of the calcium ion. The results demonstrated variations in the osteoblastic calcium signaling response between the compression and stretching stimuli. The magnitude of an increase in the intracellular calcium ion concentration is much higher in the compression stimuli-applied cell group. Treatment of calcium-free medium nearly suppressed the calcium signaling response to both types of mechanical stimulation. Thapsigargin treatment induced an increase in the magnitude of calcium signaling response to the compression stimuli, while suppressed the slow and sustained increase in the calcium ion concentration in the stretching stimuli-applied cell group. These findings demonstrate the difference in the characteristics of osteoblastic calcium signaling response between compression and stretching mechanical stimuli.

Keywords: cell biomechanics, MEMS, calcium signaling, mechanical stimuli, osteoblast

1. Introduction

In orthodontics, an orthodontic appliance applies a continuous force to the tooth and causes tooth movement. During tooth movement, opposing bone metabolism mechanisms occur in the periodontal ligament. Bone resorption and formation occur in areas where compressive and tensile forces act, respectively [1, 2]. However, the mechanisms underlying these variations in bone metabolism remain unclear. This study aimed to investigate the differences in the osteoblasts, bone-forming cells, and their response characteristics to compression and stretching stimuli. Osteoblasts alter their intracellular Ca^{2+} concentration ($[Ca^{2+}]_i$) in response to mechanical stimuli; this is known as the intracellular calcium signaling response. $[Ca^{2+}]_i$ plays an important role as a trigger element for biochemical signals and encodes mechanical stimulus information for biochemical signaling [3–5]. Various characteristics of intracellular calcium signaling, such as the magnitude, frequency, duration, and rate of increase, include biochemical signal information. In addition, two main calcium ion sources are known for their intracellular calcium signaling responses. One is the influx from outside the cell through channels in the plasma membrane, and the other is the release from intracellular calcium stores. To understand the mechanism of calcium signaling responses to stimuli, it is important to understand which of these calcium ion sources are involved.

In this study, we investigated the effects of mechanical stimulation using compression and tension on the calcium signal response characteristics of osteoblasts. For the compression stimulus, a glass microneedle was directly indented onto the cell, and for the tensile stimulus, a substrate stretch was applied using the originally developed cell-stretching MEMS device. We also investigated the contributions of intracellular calcium stores and extracellular calcium to the osteoblastic calcium signaling response to two types of mechanical stimuli. We prepared three cell groups: i) no-treatment group as a control, ii) thapsigargin-treated group to deplete Ca^{2+} in the endoplasmic reticulum (ER), and iii) Ca^{2+}-free medium group in which Ca^{2+} was chelated using GEDTA. We observed and evaluated the change in $[Ca^{2+}]_i$ as a response to two types of mechanical stimulation using the ratiometry method with two fluorescent dyes: Ca^{2+} indicator Fluo-8H and cytosolic labeling calcein red-orange. We measured two characteristics of the calcium signaling response quantitatively: the maximum increasing magnitude of $[Ca^{2+}]_i$ and the time to reach maximum $[Ca^{2+}]_i$.

We attempted to discuss the mechanism of the calcium signaling response to two types of mechanical stimuli based on these results.

2. Materials and Methods

2.1. Cell Culture and Fluorescent Labeling

The mouse osteoblast cell line MC3T3-E1 was provided by the RIKEN BRC through the National Bio-Resource Project of the MEXT, Japan. Cells were cultured in α-MEM (Wako) containing 10% FBS (Gibco) and maintained in 5% CO_2 at 37°C. Prior to the experiment, cells were seeded onto a fibronectin (Sigma-Aldrich)-coated 35 mm glass bottom dish with a built-in cell stretching microdevice developed by the authors at a cell density of approximately 5.0×10^4 cells/dish. For the fibronectin coating, a solution prepared at 5 μg/cm^2 was used and stored at room temperature for 1 h. The coated glass-bottomed dishes were rinsed twice with PBS. After 18 h of preincubation for sufficient cell adhesion, the fluorescent Ca^{2+} indicator Fluo-8H and the labeling reagent calcein red-orange were loaded into the cells. Hank's balanced salt solution (HBSS) (Wako) containing 3 μM Fluo-8H-AM (AAT Bioquest), 4 μM calcein red-orange-AM (Molecular Probes), and 0.1% Pluronic F-127 (Life Technologies) was used as the loading buffer. Fluo-8H increases the fluorescent intensity as the Ca^{2+} concentration increases. In contrast, calcein red-orange maintains its fluorescence regardless of the Ca^{2+} concentration. To calculate the ratio of fluorescent intensities (Fluo-8H / calcein red-orange), we can evaluate the change in the intracellular Ca^{2+} concentration quantitatively and reduce the motion artifact attributed to the rigid displacement during glass microneedle indentation or stretch application. Normal culture medium was replaced by the loading buffer, and the cells were cultured for 30 min in 5% CO_2 at 37°C to load the fluorescent indicators into the cells. After loading the indicator, the cells were rinsed twice with PBS (Wako), and the loading buffer was replaced with an imaging buffer and used for fluorescent image acquisition. Thapsigargin (50 nM) was added to the loading and imaging buffers to inhibit ER activity. Thapsigargin is a non-competitive inhibitor of ER Ca^{2+} ATPase that blocks the ability of cells to pump calcium ions into the ER. Thapsigargin treatment depletes calcium ion in the ER. Calcium-free DMEM (supplemented with 2 mM GEDTA) was used as a Ca^{2+}-free medium to inhibit Ca^{2+} influx from the extracellular medium into cells.

2.2. Mechanical Stimuli Application

A glass microneedle was used to apply indentation stimuli. The tip of the microneedle with a diameter of approximately 10 mm was processed by heat policing to make it smooth and round to protect the cells from damage. The microneedle was attached to a micromanipulator as shown in **Fig. 1**, and the tip was placed on a cell to apply the indentation stimuli. The indentation speed was low, and it took approximately 10 s from start to end. After completion of the indentation, the glass needle was held in the same position and the indentation was continued until the end of the observation. The indentation depth was limited to the focal plane. The position of the focal plane was approximately 5 μm above the cell base, and the microneedle indentation did not cause damage to the cell nucleus or cell membrane. **Figs. 2** and **3** show a schematic illustration (from side view) and bright-field image (from top view) of the direct indentation of the glass microneedle onto the cell, respectively.

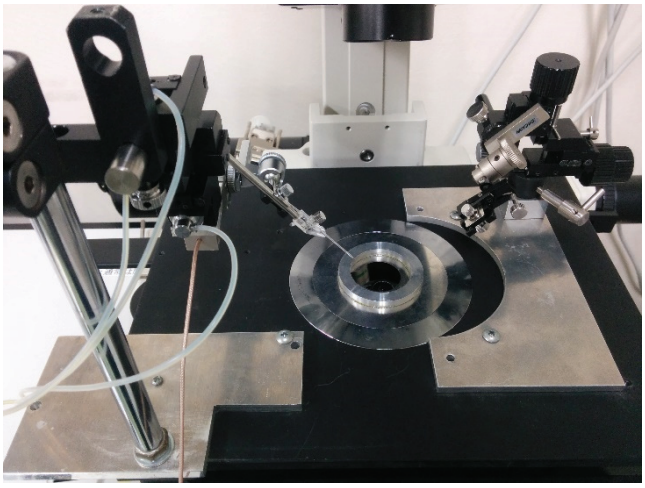

Fig. 1. A glass microneedle mounted on the micromanipulator.

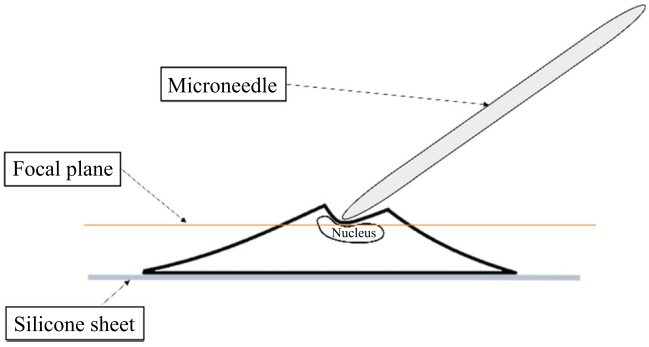

Fig. 2. Schematic illustration of direct indentation of the glass microneedle onto the cell (side view).

A cell-stretching MEMS device developed by the authors was used to apply the stretching stimuli. The device was slightly modified based on that of a previous study [6]. **Fig. 4** shows a schematic diagram of the microdevice. Six microdevices were fabricated on a 22 mm square cover glass, and the cover glass was attached to a 35-mm dish with ϕ18-mm hole at the bottom. Each microdevice consisted of one pair of arms fabricated from photoresistant SU-8 and a cell-stretching sheet fabricated from a silicone elastomer. Two metal needles were placed on each arm, as shown in **Fig. 5**. The needle on the right side was held by the micromanipulator via a piezoelectric actuator (MC-140L, Mess-Tek) to apply a uniaxial stretch to the other end of the sheet with a well-controlled strain

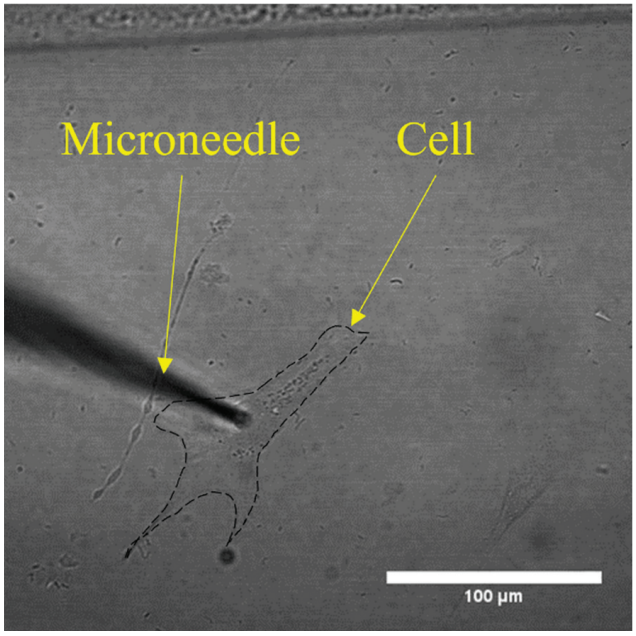

Fig. 3. Bright field image of direct indentation of the glass microneedle onto the cell (top view).

magnitude and strain rate. In this study, a uniaxial strain of 10% was applied to the cells at a constant strain rate of 20%/s. The strain magnitude was estimated by measuring the deformation of the stretch chamber using the transmitted images. In this experiment, the orthogonal strain attributed to the Poisson effect was ignored.

2.3. Image Acquisition and Analysis

Fluorescent images of the Ca^{2+} indicators and labeling reagents were obtained using an inverted confocal laser scanning microscope (A1R, Nikon) with ×60 oil immersion objective lens. As shown in **Fig. 6**, Fluo-8H and calcein red-orange were excited by a 488 nm laser and 561 nm laser, respectively, and their fluorescence was split using a 525 nm and 700 nm band-pass filter with a 50 nm bandwidth, respectively. Three images each of Fluo-8H fluorescence, calcein red-orange fluorescence, and transmitted images were acquired simultaneously using three independent photomultiplier tubes. The recorded image size was 512×512 pixels with 12-bit resolution. The image acquisition rate was approximately 3.73 frames/s (averaged from eight images to reduce noise). Each image acquisition time was 2.5 min long, consisting of an initial 0.5 min basal period without any stimulus application, followed by a 2 min mechanical stimulation (indentation or stretching) period. All the experiments were conducted in normal atmosphere and at room temperature (25°C–27°C). Even though indentation stimulation was conducted, cells that existed on the stretching sheet of the cell-stretching MEMS device were selected to unify the image acquisition conditions, such as fluorescence intensities and spatial resolution. The obtained images were analyzed using ImageJ software (NIH). Although the shape of the cell deformed owing to the stretch application, the average value of fluorescence intensity was calculated using the ROI defined by the initial (before stretch) outline shape of the cell. To reduce motion artifacts due to out-of-focus stretching, changes in the concentration of intercellular calcium were evaluated using ratiometric microscopy. The fluorescence ratio was defined by (Fluo-8H / calcein red-orange) and expressed as a ratio over the initial baseline for each cell. The maximum fluorescence ratio and rising time of the fluorescence ratio were also investigated for each condition. The "maximum fluorescence ratio value" was defined as the point at which the slope of five consecutive fluorescent ratio data (fluorescence ratio value/second) become 0.05 or less. The "maximum fluorescence ratio value" defined here is not the maximum value during the observation period, but the value at the point at which the rate of increase of the fluorescence ratio value reaches an inflection point and slows down. The rising time was defined as the time from mechanical stimuli application to reaching the above defined "maximum fluorescence ratio value." Some of the observed cells showed a decrease in the fluorescence ratio without an increase. These cells were excluded from the measurement of the rising time. Paired t-tests were used to compare the control group and the thapsigargin-treated group or Ca^{2+}-free medium group. Differences were considered statistically significant at $\alpha = 0.05$.

3. Results

3.1. Direct Indentation Stimuli

Figure 7 shows typical fluorescence images of osteoblasts in response to indentation stimulation. The left and right columns show the initial and post-indentation states, respectively. As shown in the figure, the needle tip shadow appeared as a spot and the Fluo-8H fluorescence intensity increased with the osteoblastic calcium signaling response. **Fig. 8** shows the time-course change in the fluorescence ratio of cells subjected to direct indentation stimuli. Number of cells in the control, thapsigargin-treated, and Ca^{2+}-free medium groups are as follows: 6, 13, and 6, respectively. In the control and thapsigargin-treated groups, all cells exhibited a significant increase in the fluorescence ratio. In the Ca^{2+}-free medium group, some cells (50%) exhibited minimal changes in the fluorescence ratio. The maximum fluorescence ratios in response to the application of the indentation stimuli are shown in **Fig. 9**. The rate of increase in $[Ca^{2+}]_i$ in the thapsigargin-treated group was approximately 2 times larger than that in the control group ($p < 0.01$). In contrast, the Ca^{2+}-free medium group was smaller than the control group ($p < 0.01$). **Fig. 10** shows the rising time of the fluorescence ratio in response to the application of the indentation stimuli. The thapsigargin-treated group required more time to reach the maximum fluorescence ratio than the control group ($p < 0.01$).

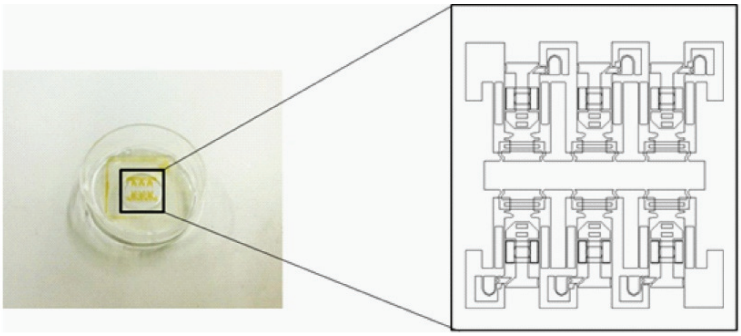

(a) Arrangement of cell stretching microdevices on the cover glass attached to 35 mm dish

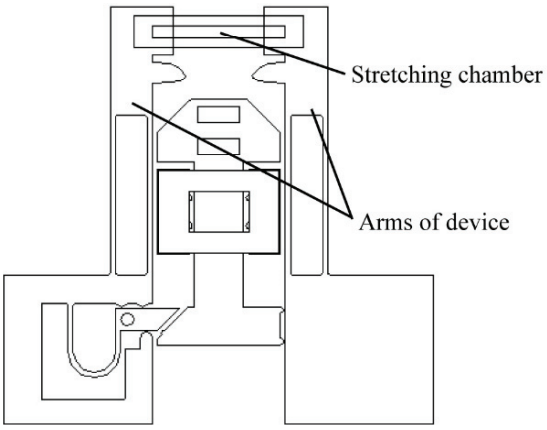

(b) Schematic of microdevice

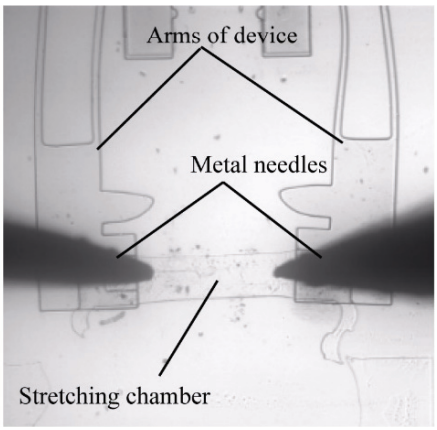

(c) Stretching set up of metal needles and microdevice

Fig. 4. Figures of the cell stretching microdevice. (a) Six microdevices were fabricated onto the cover glass. The cover glass is attached to the 35-mm dish with ϕ18-mm bottom hole. (b) Schematic of the microdevice. The microdevice consists of one pair of arms and cell stretching chamber. The overall device dimensions are roughly 2 mm $\times$ 4 mm and the stretch chamber dimensions are 800 µm $\times$ 200 µm. The thickness of the chamber sheet is 5 µm. (c) Microscopic image of the stretching set up of the microdevice. Two metal needles mounted on the micromanipulator are set onto the arms of the device. The needle on the left side is connected to a piezo electric actuator to apply uniaxial stretch to the chamber.

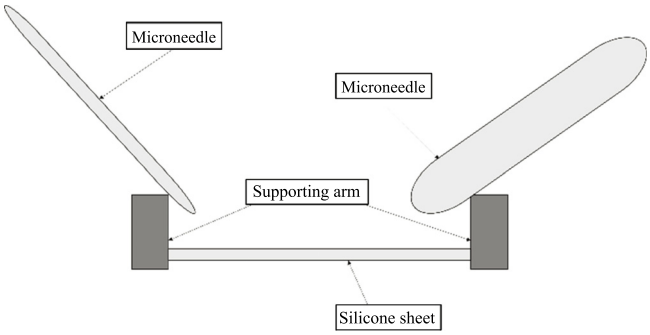

Fig. 5. Schematic illustration of applying stretch to the silicone sheet on the cell stretching MEMS device (side view).

3.2. Stretching Stimuli for Cells Substrate

Figure 11 shows the time course change in the fluorescence ratio of the cells subjected to stretching stimuli. The number of cells in the control (no-treatment group), thapsigargin-treated group, and Ca^{2+}-free medium groups are as follows: 10, 29, and 19 cells, respectively. The percentages of cells showing an increase in $[Ca^{2+}]_i$ were the control group (44%), thapsigargin-treated group (45%), and Ca^{2+}-free medium group (42%). **Fig. 12** shows the mean maximum fluorescence ratio values in the responding cells of each group. As shown in the graph, a trend towards a greater increase in the fluorescence ratio in the thapsigargin-treated group was observed; however, the difference was not statistically significant. **Fig. 13** shows the average time required to reach maximal fluorescence in each group of responding cells. Both the thapsigargin-treated and Ca^{2+}-free medium groups reached maximum fluorescence in a significantly shorter time than the control group.

4. Discussion

4.1. Calcium Response Characteristics to the Indentation Stimuli

Considering the calcium response to the indentation stimuli, a marked increase in $[Ca^{2+}]_i$ was observed in the no-treatment group and the thapsigargin-treated group, whereas in the Ca^{2+}-free group, the increase in $[Ca^{2+}]_i$

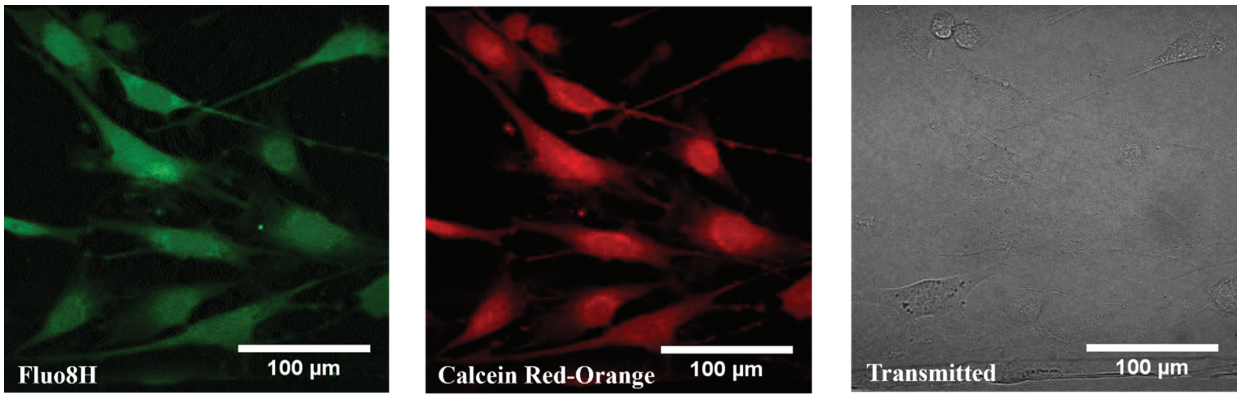

Fig. 6. Transmitted and fluorescent images of Fluo-8H and calcein red-orange in osteoblastic cells in the transparent stretching chamber (silicone sheet). The green fluorescence of Fluo-8H, the red-orange fluorescence of calcein red-orange, and the gray scale transmitted light are observed simultaneously by the three PMTs.

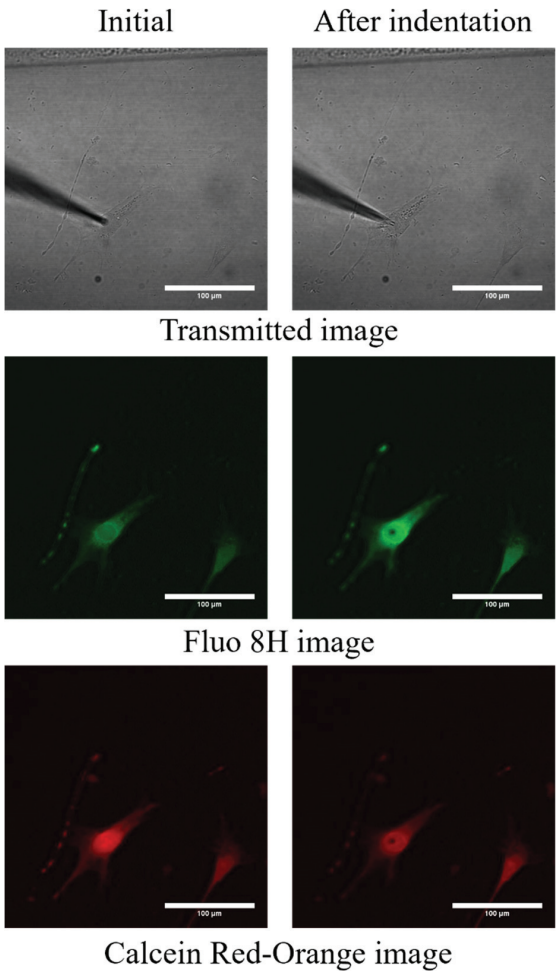

Fig. 7. Typical example of the changes in the fluorescence intensities of osteoblasts induced by indentation stimuli. The upper row shows the transmitted images, the middle row shows the Fluo-8H fluorescence images, and the lower row shows the calcein red-orange fluorescent images. The left column shows the initial state, and the right column shows the images after indentation.

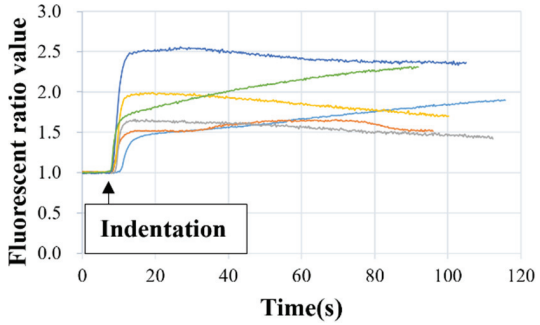

(a) No-treatment group

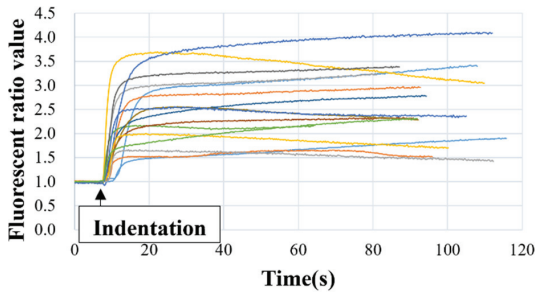

(b) Thapsigargin-treated group

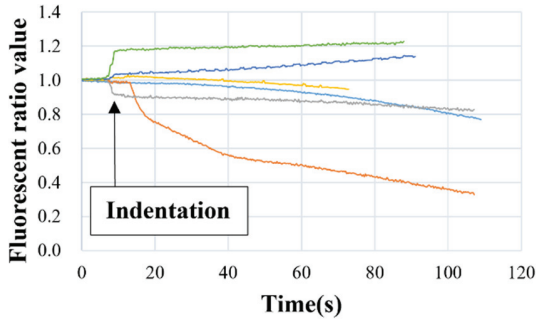

(c) Ca^{2+}-free medium group

Fig. 8. Time course changes in fluorescent intensity of the cells to which direct indentation stimuli were applied. (a) No-treatment group, (b) thapsigargin-treated group, (c) Ca^{2+}-free medium group.

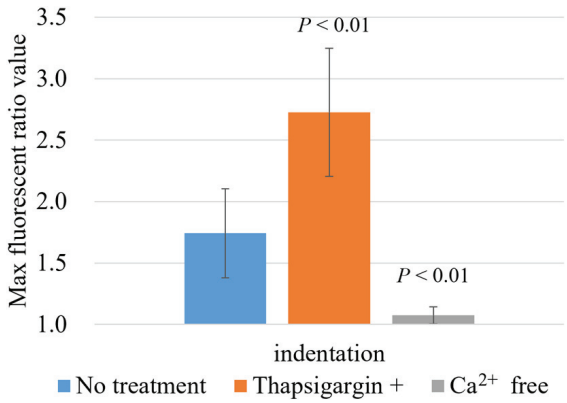

Fig. 9. Comparison of the maximum fluorescent ratio values between the three cell groups. Thapsigargin-treated group shows a greater increase in the fluorescence ratio value than the control group (no-treatment group). Ca^{2+}-free media group shows a much lesser increase.

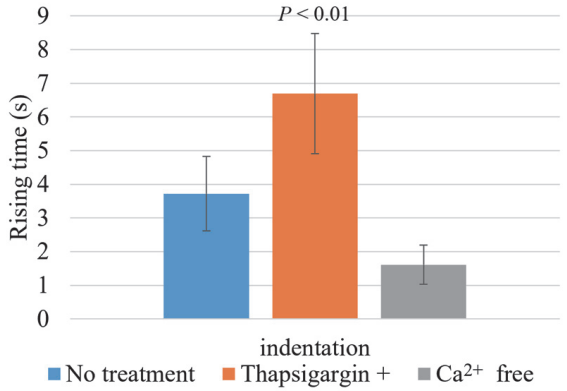

Fig. 10. Comparison of rising times between three cell groups. Thapsigargin-treated group took longer rising time than the control group.

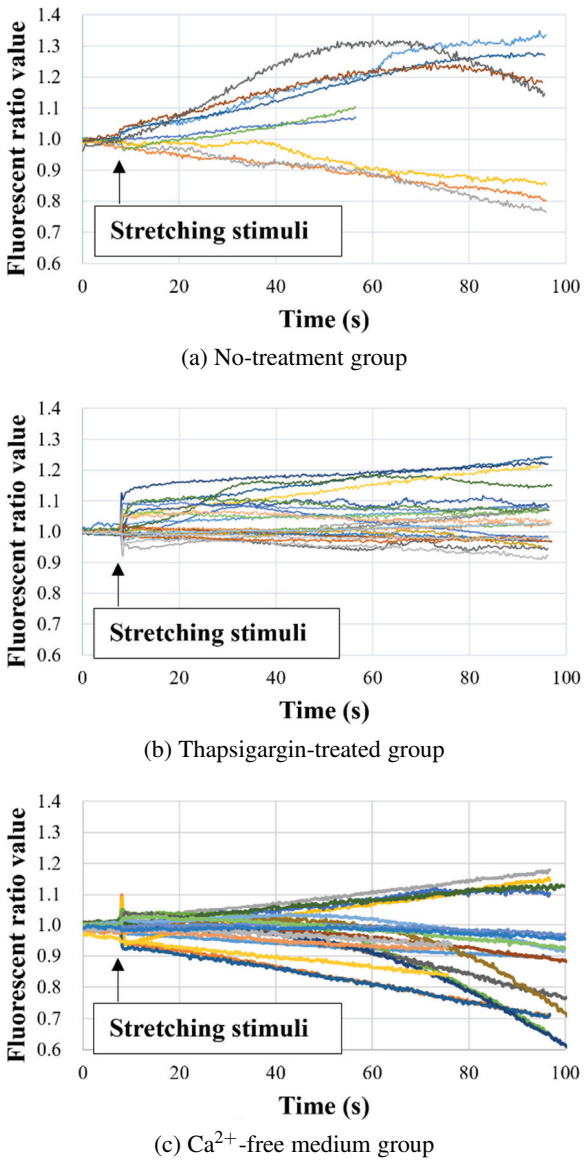

Fig. 11. Time course changes in the fluorescence ratio value of the cells which received stretching stimuli. (a) No-treatment group, (b) thapsigargin-treated group, (c) Ca^{2+}-free medium group.

was very slight but not completely suppressed. These results indicate that the source of the calcium signaling response to indentation stimuli involves both extracellular Ca^{2+} influx and release from intracellular calcium stores; however, extracellular Ca^{2+} influx is dominant.

The thapsigargin-treated group demonstrated the largest increase in $[Ca^{2+}]_i$ and the longest rising time. These results suggest that thapsigargin-induced inhibition of intracellular calcium stores inhibits the calcium induce calcium release (CICR) mechanism, resulting in only extracellular Ca^{2+} influx, which slows the rate of increase in $[Ca^{2+}]_i$. Furthermore, the inhibition of intracellular calcium stores inhibits the homeostatic mechanism that attempts to maintain a constant $[Ca^{2+}]_i$. Thus, thapsigargin treatment inhibited calcium ion uptake into the ER and weakened its ability to reduce $[Ca^{2+}]_i$, resulting in the largest increase in $[Ca^{2+}]_i$. The lack of a coordinated release from calcium stores and the inability of the intracellular calcium ion homeostasis mechanism to operate resulted in a higher upper limit of ion concentration, which may have contributed to the longer rising time.

4.2. Calcium Response Characteristics to Stretching Stimuli

Not all cells loaded with stretching stimuli demonstrated a calcium signaling response. The response rates were 44%, 45%, and 42% in the no-treatment, thapsigargin-treated, and Ca^{2+}-free groups, respectively. These results suggest that the rate of the cellular response to stretch stimuli is not affected by the source of the calcium ions. The same was true for the increase in the calcium ion concentrations; although the thapsigargin-treated group tended to have a higher increase, no statistically significant difference was observed in the increase in calcium ion concentrations among the three groups. These results suggest that the influx of calcium ions from outside the cell and their release from calcium stores may contribute equally to stretching stimulation.

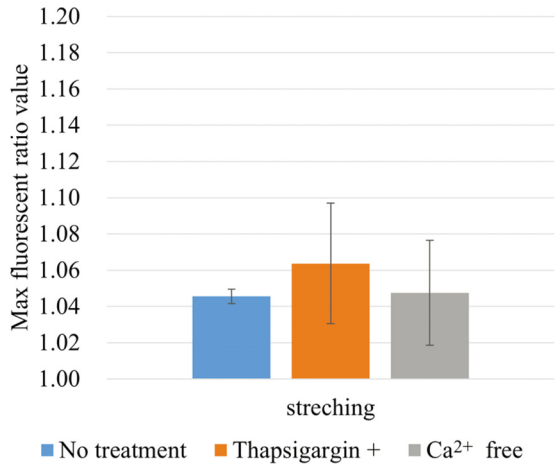

Fig. 12. Comparison of the maximum fluorescence ratio values between the three cell groups. There was a trend towards greater maximal fluorescence ratio value in the thapsigargin-treated group, but this was not statistically significant.

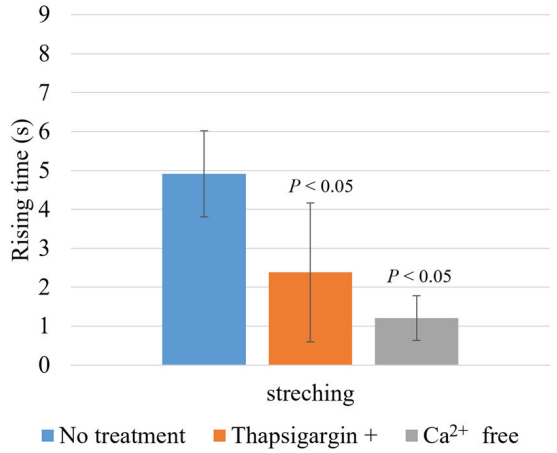

Fig. 13. Comparison of the rising times between the three cell groups. The time to reach the maximum fluorescence ratio value was shorter in the thapsigargin-treated group and the Ca^{2+}-free medium group than in the control group.

However, the time to reach the peak concentration varied greatly among the three groups. The amplification of the increase in the calcium concentration by CICR may vary in response to the stretching stimuli. In combination with the results of the indentation experiments, it may be necessary to conduct observations for longer periods of time and include not only the increase in $[Ca^{2+}]_i$ but also the decrease and return to the steady state to better understand the mechanism of intracellular calcium homeostasis in osteoblasts in response to mechanical stimuli.

4.3. Comparison of Calcium Response Characteristics to Indentation and Stretching Stimuli

Comparing the indentation and stretching stimuli in the no-treatment group, the response to the indentation stimulus was clearly greater in terms of the increase in $[Ca^{2+}]_i$. Furthermore, nearly all the cells responded to the indentation stimulus, whereas only approximately 40% of the cells responded to the stretching stimulus. One possible reason is that the indentation stimulus causes a very localized and large deformation (including bending and stretching) of the plasma membrane around the needle tip, resulting in a very strong activation of the stretch-activated (SA) channels [7]. In contrast, the force produced by the stretching stimulus at the focal adhesion is relatively weak and may not be strong or frequent enough to activate the SA channels around the focal adhesion or the plasma membrane connected to the actin cytoskeleton. However, attributing this result to simple differences in the manner in which compression and tension are applied is challenging. In the present study, the stretching stimulus stretched the entire substrate to which the cells were attached, whereas the indentation stimulus produced localized compressive and bending deformations in the plasma membrane. It was not possible to directly compare the forces produced in the focal adhesions by the stretching stimulus with the compressive and bending stresses produced by the indentation stimulus. This is a limitation of the stimulation technique employed in this study.

However, the calcium signal response characteristics possibly vary between tension and compression, as the change in the rate of increase in $[Ca^{2+}]_i$ when calcium stores were inhibited was the exact opposite between the indentation and stretching stimuli.

5. Conclusions

In this study, we investigated the differences in the characteristics of calcium signaling responses by applying two types of mechanical stimuli to osteoblasts: compressive stimulus by direct microneedle indentation, and stretching stimulus by an originally developed MEMS device. The results demonstrated that osteoblasts showed relatively strong calcium responses to indentation stimulus. The source of the increase in intracellular calcium ion concentration was mostly calcium influx from outside the cell, and the contribution of the release from intracellular calcium stores was small. In contrast, osteoblasts demonstrated a relatively weak calcium response to the stretching stimuli. The source of calcium was shown to be the influx of extracellular calcium and release from intracellular calcium stores, with equal contributions. These results suggest that osteoblasts exhibit different calcium signaling responses to different types of mechanical stimuli. This study may provide insights into the mechanisms underlying the opposing bone metabolism patterns of bone resorption and bone formation in orthodontic bone remodeling.

Acknowledgments

This study was supported by the Support Center for Advanced Medical Sciences at Graduate School of Biomedical Sciences,

Tokushima University. We would like to express our gratitude to Mr. Ryuta Yasui, a graduate student, who assisted with conducting this study.

References:

[1] C. Verna, M. Dalstra, and B. Melsen, "The rate and the type of orthodontic tooth movement is influenced by bone turnover in a rat model," European J. Orthodontics, Vol.22, Issue 4, pp. 343-352, 2000. https://doi.org/10.1093/ejo/22.4.343

[2] A. V. Schepdael, J. V. Sloten, and L. Geris, "A mechanobiological model of orthodontic tooth movement," Biomech. Modeling in Mechanobiol., Vol.12, No.2, pp. 249-265, 2013. https://doi.org/10.1007/s10237-012-0396-5

[3] L. M. Godin, S. Suzuki, C. R. Jacobs, H. J. Donahue, and S. W. Donahue, "Mechanically induced intracellular calcium waves in osteoblasts demonstrate calcium fingerprints in bone cell mechanotransduction," Biomech. Modeling in Mechanobiol., Vol.6, No.6, pp. 391-398, 2007. https://doi.org/10.1007/s10237-006-0059-5

[4] S. W. Donahue, C. R. Jacobs, and H. J. Donahue, "Flow-induced calcium oscillations in rat osteoblasts are age, loading frequency, and shear stress dependent," Am. J. Physiol. Cell Phisiol., Vol.281, No.5, pp. C1635-C1641, 2001. https://doi.org/10.1152/ajpcell.2001.281.5.C1635

[5] M. Zayzafoon, "Calcium/calmodulin signaling controls osteoblast growth and differentiation," J. Cellular Biochem., Vol.97, No.1, pp. 56-70, 2006. https://doi.org/10.1002/jcb.20675

[6] K. Sato, S. Kamada, and K. Minami, "Development of microstretching device to evaluate cell membrane strain field around sensing point of mechanical stimuli," Int. J. Mech. Sci., Vol.52, No.2, pp. 251-256, 2010. https://doi.org/10.1016/J.IJMECSCI.2009.09.021

[7] K. Naruse and M. Sokabe, "Involvement of stretch-activated ion channels in Ca^{2+} mobilization to mechanical stretch in endothelial cells," Am. J. Phisiol. Cell Phisiol., Vol.264, No.4, pp. C1037-C1044, 1993. https://doi.org/10.1152/ajpcell.1993.264.4.C1037

Name:
Katsuya Sato

Affiliation:
Associate Professor, Graduate School of Technology, Industrial and Social Sciences, Tokushima University

Address:
2-1 Minamijosanjima, Tokushima 770-8506, Japan

Brief Biographical History:
2005- Assistant Professor, Yamaguchi University
2009- Lecturer, Tokushima University
2020- Associate Professor, Tokushima University

Main Works:
• "Development of vibration mechanical stimuli loading device for live cell fluorescence microscopy," J. of Biomechanical Science and Engineering, Vol.17, No.2, 2022.

Membership in Academic Societies:
• The Japanese Society of Mechanical Engineers (JSME)
• Japanese Society for Medical and Biological Engineering (JSMBE)
• The Biophysical Society of Japan (BSJ)

Name:
Tasuku Nakahara

ORCID:
0000-0001-8969-2776

Affiliation:
Associate Professor, Graduate School of Sciences and Technology for Innovation, Yamaguchi University

Address:
2-16-1 Tokiwadai, Ube, Yamaguchi 755-8611, Japan

Brief Biographical History:
2012 Received M.Eng. degree from Kagawa University
2015 Received D.Eng. degree from Kyoto University
2015- Assistant Professor, Yamaguchi University
2022- Associate Professor, Yamaguchi University

Main Works:
• T. Nakahara, K. Ise, and K. Minami, "Fabrication of thermally actuated microheater with SU-8/Cu composite," J. of Micromechanics and Microengineering, Vol.31, Article No.095007, 2021.

Membership in Academic Societies:
• The Japan Society of Mechanical Engineers (JSME)
• The Institute of Electrical Engineers of Japan (IEEJ)
• The Society for Chemistry and Micro-Nano Systems (CHEMINAS)

Name:
Kazuyuki Minami

Affiliation:
Professor, Graduate School of Sciences and Technology for Innovation, Yamaguchi University

Address:
2-16-1 Tokiwadai, Ube, Yamaguchi 755-8611, Japan

Brief Biographical History:
1985 Received M.Eng. degree from Tohoku University
1985- Olympus Optical Co., Ltd.
1990- Research Associate, Tohoku University
1994 Received D.Eng. degree from Tohoku University
1994- Lecturer, Tohoku University
1999- Associate Professor, Yamaguchi University
2003- Professor, Yamaguchi University

Main Works:
• "Development of micro mechanical device having two-dimensional array of micro chambers for cell stretching," Biomedical Microdevices, Vol.20, Issue 1, Article No.10, 2018. https://doi.org/10.1007/s10544-017-0256-2

Membership in Academic Societies:
• The Japan Society of Mechanical Engineers (JSME)
• The Institute of Electrical Engineers of Japan (IEEJ)
• Japanese Society for Medical and Biological Engineering (JSMBE)
• The Japan Society for Precision Engineering (JSPE)
• The Japan Society of Applied Physics (JSAP)